Journal of the Korean Astronomical Society
50: 111 ∼ 124, 2017 August

https://doi.org/10.5303/JKAS.2017.50.4.111
pISSN: 1225-4614 · eISSN: 2288-890X
http://jkas.kas.org

Morphology of Dwarf Galaxies in Isolated Satellite Systems

Hong Bae Ann
Pusan National University, 2 Busandaehak-ro, Geumjeong-gu, Busan 46241, Korea; hbann@pusan.ac.kr

Received May 22, 2017; accepted July 18, 2017

Abstract: The environmental dependence of the morphology of dwarf galaxies in isolated satellite systems is analyzed to understand the origin of the dwarf galaxy morphology using the visually classified morphological types of 5836 local galaxies with $z \lesssim 0.01$. We consider six sub-types of dwarf galaxies, dS0, dE, dE$_{bc}$, dSph, dE$_{blue}$, and dI, of which the first four sub-types are considered as early-type and the last two as late-type. The environmental parameters we consider are the projected distance from the host galaxy (r_p), local and global background densities, and the host morphology. The spatial distributions of dwarf satellites of early-type galaxies are much different from those of dwarf satellites of late-type galaxies, suggesting the host morphology combined with r_p plays a decisive role on the morphology of the dwarf satellite galaxies. The local and global background densities play no significant role on the morphology of dwarfs in the satellite systems hosted by early-type galaxies. However, in the satellite system hosted by late-type galaxies, the global background densities of dE and dSph satellites are significantly different from those of dE$_{bc}$, dE$_{blue}$, and dI satellites. The blue-cored dwarf satellites (dE$_{bc}$) of early-type galaxies are likely to be located at $r_p > 0.3$ Mpc to keep their cold gas from the ram pressure stripping by the hot corona of early-type galaxies. The spatial distribution of dE$_{bc}$ satellites of early-type galaxies and their global background densities suggest that their cold gas is intergalactic material accreted before they fall into the satellite systems.

Key words: galaxies: general — galaxies: morphology — galaxies: dwarfs

1. Introduction

Dwarf galaxies are the most dominant populations of the nearby universe ($z \lesssim 0.01$) as well as the building blocks of massive galaxies in the ΛCDM cosmology. There are two types of dwarf galaxies: dwarf elliptical-like galaxies (dEs) and dwarf irregular galaxies (dI). The dEs include dS0, dE, dSph, dE$_{bc}$ and dE$_{blue}$ (Ann et al. 2015). The dE$_{bc}$ represents dE galaxies with blue cores and the dE$_{blue}$ represents globally blue dwarf galaxies that have ellipsoidal shapes. Like the blue elliptical galaxies (Strateva et al. 2001), dE$_{bc}$ and dE$_{blue}$ can be distinguished from other dEs by the colors, not by the shapes. The dSph is not always distinguished from the dE in literature (Sandage & Binggeli 1984; Ferguson & Binggeli 1994) but most previous studies recognize the dSph galaxy as a distinct class of galaxies (Mateo 1998; Gallagher & Wyse 1994; Grebel 1997; van den Bergh 1999).

The morphology of a dwarf galaxy is easily affected by its environment because of its small mass. The environmental quenching, a sudden shutdown of star formation driven by the environment, is most pronounced for the dwarf galaxies in groups and clusters (Peng et al. 2010, 2012; Kovac et al. 2014; Tal et al. 2014; Wetzel et al. 2015). This is the reason why environmental quenching is sometimes termed satellite quenching. There are several mechanisms proposed for environmental quenching (see Boselli & Gavazzi 2006, for a review). This quenching is most effective in cluster galaxies because the density and temperature of the intracluster medium is high enough to remove gas from late-type galaxies by ram pressure stripping (Gunn & Gott 1972; Roediger & Hensler 2005; Jachym et al. 2007; Boselli et al. 2008; McCarthy et al. 2008; Tonnesen & Bryan 2009; Bekki 2009; Vollmer 2009; Book & Benson 2010; Tecce et al. 2010; Kimm et al. 2011; Vijayaraghavan & Ricker 2015; Zinger et al. 2016) and tidal interactions among galaxies are expected to be frequent enough to transform their morphology via galaxy harassment (Moore et al. 1998). Morphology transformation by harassment is not effective in poor groups and satellite systems because encounters among satellite galaxies are too rare to perturb their mutual orbits (Mayer et al. 2001; Pasetto et al. 2003). However, ram pressure stripping seems to be operating in poor groups and satellite systems (Marcolini et al. 2003; Hester 2006; Rasmussen et al. 2006; Kawata & Mulchaey 2009; Gatto et al. 2013; Fillingham et al. 2016; Emerick et al. 2016; Brown et al. 2017).

The correlation between the observed properties such as morphology, colors, and star formation rate of central galaxies and their neighbors, dubbed "galactic conformity", is now well established (Weinman et al. 2006; Ann et al. 2008; Kauffmann et al. 2013). In particular, Ann et al. (2008) found the morphology conformity between an isolated host and its satellites using morphology itself rather than proxies of galaxy morphology such as colors and star formation rate (Weinman et al. 2006; Kauffmann et al. 2013). The morphology conformity is thought to be a result of morphology transformation driven by environmental quenching

Corresponding author: H. B. Ann

which leads to a higher fraction of early-type satellites near early-type hosts than late-type hosts. The main mechanism of the environmental quenching in satellite systems that drives the morphology conformity is the ram pressure stripping. It is more effective in early-type hosts because the hot corona of an early-type galaxy is larger than that of a late-type galaxy (Jeltema et al. 2008; O'Sullivan et al. 2001; Mulchaey & Jeltema 2010; Rasmussen et al. 2009). Recent models for satellite infall and ram pressure stripping (Slater & Bell 2014) show that quenching occurs within $\sim$ 2Gyr for low-mass satellites while massive satellites continue to form stars for a prolonged time, $>$ 5Gyr after falling into their host. Their models are consistent with the observations of the local group (LG) that nearly all the dwarf galaxies with $M_{star} \lesssim 10^9 M_\odot$ within 300 kpc from the Milky Way and M31 show no star formation (Wetzel et al. 2015).

In order to transform late-type galaxies into early-type ones, quenching of star formation is not sufficient. It should accompany structural changes, from disks to spheroidals, if dE and dSph galaxies are transformed from late-type disk galaxies. In satellite systems, tidal stirring by the host galaxy plays a major role to transform dwarf irregular galaxies into dwarf spheroidal galaxies (Mayer et al. 2001, 2006; Lokas et al. 2010; Yozin & Bekki 2015). In cluster environment, harassment (Moore et al. 1998) and tidal shock (Mayer et al. 2001) are responsible for the structural changes after satellite galaxies enter into clusters or satellite systems. Tidal shocks also play some role in removing the cold gas from satellite galaxies (Mayer et al. 2006) but complete removal of cold gas requires hydrodynamical processes such as ram pressure stripping (Gunn & Gott 1972).

Since the morphology of a galaxy depends on the environment where it forms, we expect a close relationship between the satellite morphology and its environment, parameterized by the local and global background densities as well as the projected distance from the host galaxy (r_p) and the host morphological type. It is of interest to see whether the spatial distributions of dwarf satellites can be distinguished by their subtypes. Until now, there is no detailed study on the environment of dwarf galaxies, except for those in the Local Group (van den Bergh 1994), local volume within 10 Mpc (Karachentsev et al. 2014) and the Virgo cluster (Lisker et al. 2007). The reason for the limited number of studies on the environment of the dwarf galaxies is that there is no redshift survey to cover the faint dwarf galaxies before the Sloan Digital Sky Survey (SDSS; York et al. 2000).

In this regard, this study seeks to find some clues about the origin of dwarf galaxies by examining the spatial distributions of satellite galaxies in the isolated satellite systems where the ram pressure from the hot intergalactic medium is thought to be too weak to completely remove the cold gas in late-type galaxies because isolated satellite systems are likely to be located in the low-density regions. If the morphology of a galaxy can be transformed after it becomes a satellite galaxy, we expect some correlations between satellite morphology and the distance from the host galaxy because tidal and hydrodynamical interactions depend on the distance between the host and its satellite. Of course, in cases where morphology transformation is still in progress, they are likely to be located in the outlying regions of satellite systems. The rotationally supported dE galaxies which are located in the outer parts of the Virgo cluster (Toloba et al. 2011) may be examples of dE galaxies transformed from late-type disk galaxies. Benson et al. (2015) showed that tidally stirred dE galaxies with significant rotation are located in the outer parts of the model clusters.

The dE$_{bc}$ galaxy is of special interest. The pronounced feature distinguishing dE$_{bc}$ galaxies from other dEs is the blue core where active star formation is supposed to be taking place, suggesting the presence of cold gas there. Then, what is the origin of the cold gas? It could be the intergalactic material accreted onto a dE satellite or leftover material after being transformed from late-type galaxies. It is also possible that the cold gas of a late-type host can be transferred to a dE to make a dE$_{bc}$. There are no simulations to predict such a cold gas transfer from a late-type host to its satellite although hydrodynamical simulations, e.g., distant encounter models of Hwang & Park (2015), show that cold gas in a late-type galaxy can be transferred to the center of an early-type galaxy whose mass is comparable to the late-type galaxy. We will explore the origin of the cold gas in dE$_{bc}$ satellites by analyzing their environment.

This paper is organized as follows. The data and sample selection are described in Section 2 and the results of the present study are given in Section 3. Summary and discussion on the origin of the dwarf galaxy morphology are given in the last section.

2. DATA AND SAMPLE SELECTION

2.1. Morphological Types of Dwarf Galaxies

We used the galaxies in the Catalog of Visually Classified Galaxies in the nearby universe (CVCG; Ann et al. 2015) as the primary sample of the present study. The basic source of data in the CVCG is the Korea Institute of Advanced Study Value-Added Galaxy Catalog (KIAS-VAGC; Choi et al. 2010) which provides photometric and spectroscopic data derived from the SDSS Data Release 7 (Abazajian et al. 2009). They supplemented spectroscopic redshifts of galaxies brighter than the magnitude limit ($r_{petrosian} \sim 14.5$) of the target galaxies of the SDSS spectroscopic observation from various redshift catalogs. Ann et al. (2015) added faint galaxies from the NASA Extragalactic Data Base (NED) and the galaxies in Makarov & Karachentsev (2011) that are not overlapped with the galaxies from the KIAS-VAGC. These supplements make the CVCG nearly complete to galaxies brighter than $r_{petrosian} = 17.77$.

The detailed description of the morphological properties of dwarf galaxies is given in Ann et al. (2015)

but here we describe the morphology of dwarf galaxies briefly. For three sub-types of dE-like galaxies (dS0, dE, dSph), the presence/absence of nucleation is distinguished by the subscript 'n' and 'un'. For example, the dE_n galaxy represents the dE galaxy with nucleation while dE_{un} denotes the dE galaxy with no nucleation. However, we do not distinguish nucleated dwarfs from un-nucleated ones in the present study because of the small sample size of the dwarf satellites.

Figure 1 shows the prototypical images of the dwarf elliptical-like galaxies. As can be seen in the first and second rows of Figure 1, dS0 and $dS0_p$(peculiar dwarf lenticulars) galaxies are characterized by the lens-like features in the central regions. Some of them show signatures of spiral arm remnant in the outer part of the disk (Jerjen et al. 2000; Barazza et al. 2002; Geha et al. 2003; Graham et al. 2003; de Rijcke et al. 2003; Lisker et al. 2006; Lisker 2009; Janz et al. 2012). DS0 with spiral arms are denoted as $dS0_p$ to distinguish them from the normal dS0s. Because of the small number, we do not distinguish dS0 and $dS0_p$ in the analysis of the correlation between the satellite morphology and environment. The dE galaxies in the third row of Figure 1 show the basic morphological properties of the dwarf elliptical-like galaxies, characterized by the elliptical shape, shallow surface brightness gradient, presence/absence of nucleation, and some signatures of spiral arm remnant (in the third column). The dE_{bc} galaxies in the fourth row are characterized by the blue core which manifests the presence of young stellar populations there. Except for the blue core, they are almost identical to dE galaxies. While the dE_{bc} galaxies show blue colors in the core only, the colors of the dE_{blue} galaxies are globally blue, similar to that of dwarf irregular (dI) galaxies. As shown in the 6th row of Figure 1, the dE_{blue} galaxies have round shapes resembling the HII region-like blue compact dwarfs (BCDs) in appearance. But their colors are less bluer than BCDs, implying less star formation. The dE_{blue} and BCD can be classified as the same type if BCDs embedded in amorphous irregular galaxies are excluded. The dSph galaxies look similar to dE galaxies but they are less luminous and somewhat bluer than dE galaxies. Because of the similar morphology of dE and dSph galaxies, they are often used interchangeably in the literature. From a photometric point of view, their colors are similar to each other but dE is slightly brighter than dSph. However, from the kinematic point of view, dE galaxies are mostly supported by rotation (Davies et al. 1983; Pedraz et al. 2002) while dSph galaxies are supported by dispersion (Geha et al. 2002).

We used galaxy distances derived from the redshifts corrected for the motion relative to the centroid of the LG using the prescription of Mould et al. (2000). If NED provides galaxy distances determined from the distance indicators, these distances were used. The number of galaxies with their distances from distance indicators is 1548. The galaxies lying inside a 10°-cone around M87 with a redshift less than $z = 0.007$ (Kraan-Korteweg 1986) are assumed to be the members of the Virgo Cluster, and we used the distance of the Virgo cluster for these galaxies. We assumed the Virgo distance as $D = 16.7$ Mpc and H=75 km s^{-1} Mpc^{-1}.

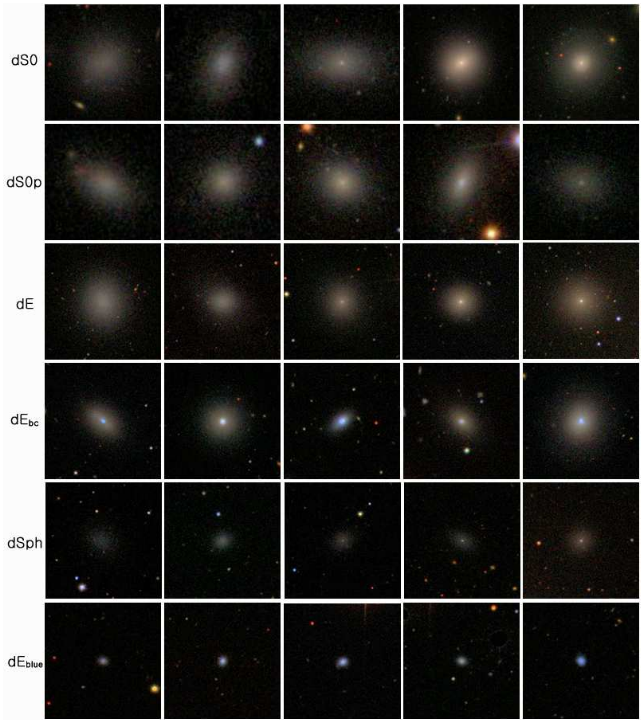

Figure 1. Sample images of dwarf elliptical-like galaxies. For dS0 ($dS0_p$), dE, and dSph galaxies, galaxies with no nucleation are displayed in the first two columns from the left.

Figure 2 shows the histograms of M_r of six sub-types of dwarf galaxies in the CVCG. We derived M_r from the r-model magnitude corrected for the extinction in the Galaxy using the r-band extinction given in the SDSS DR7. We did not apply K-correction and evolution correction. As can be seen in Figure 2, the luminosity distributions of the six sub-types of dwarf galaxies are quite different. Four of them (dS0, dE, dE_{bc} and dI) show skewed distribution with different peak luminosities and the two (dSph and dE_{blue}) show a roughly Gaussian shape. The majority of dwarf galaxies are fainter than $M_r = -17$ with some fractions of galaxies brighter than $M_r = -17$ in dS0 (15%), dE (10%) and dE_{bc} (16%) galaxies. The reason for the high fraction of bright galaxies ($M_r < -17$) in dE_{bc} galaxies is due to the presence of the bright blue cores. There is a significant difference in the luminosity distributions between dE and dSph galaxies. On average, dE galaxies are ~ 1.5 mag brighter than dSph galaxies.

2.2. Selection of Isolated Satellite Systems

A galactic satellite system which consists of a host and its satellites is said to be isolated if its host galaxy is isolated. The host galaxy of an isolated satellite system, sometimes called a central galaxy, is the most massive galaxy in the satellite system which has no companion galaxy that has a comparable mass. An isolated satellite system can be a part of a group or the group itself

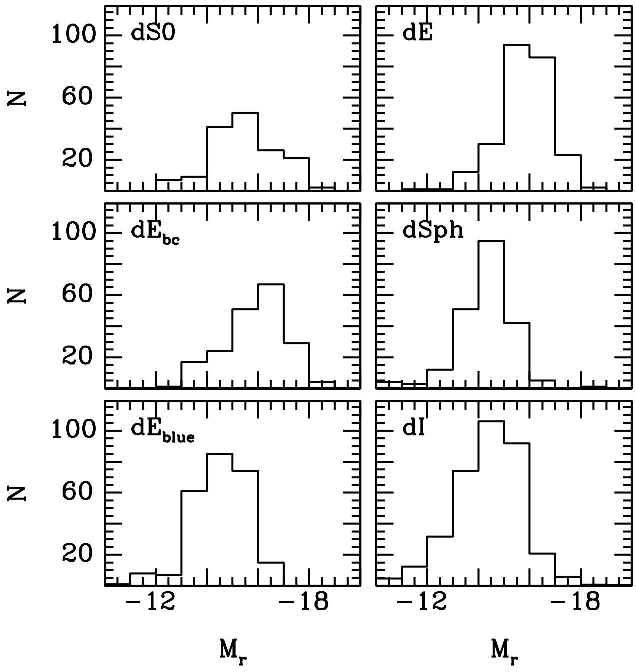

Figure 2. Luminosity distributions of six sub-types of dwarf galaxies. In case of dI galaxies, the numbers of galaxies in each luminosity bin are one fourth of the observed numbers of galaxies in each bin.

depending on the definition of group and isolation criteria. In this sense, the definition of an isolated satellite system adopted in this study is nearly the same as that of the group used by Tully (2015). However, the isolation criteria are not unique in the literature. They depend on how to define neighbor galaxies that have a comparable luminosity, $\delta M = 1 \sim 2$mag.

In most cases, neighbor galaxies are defined by two parameters, linking distance (LD) and linking velocity (ΔV^*). The LD is the maximum projected separation between a target galaxy and its neighboring galaxy and ΔV^* is the maximum radial velocity difference relative to the target galaxy. Most previous works used a fixed LD such as 0.5 Mpc and 1 Mpc (McKay et al. 2002; Prada et al. 2003; Sales & Lambas 2004; van den Boschh 2004, 2005; Zenter et al. 2005; Chen et al. 2006; Sales et al. 2007). We use variable LD following Ann et al. (2008) who defined LD as the sum of the virial radii of host and its neighbor galaxy. One of the merits using the sum of the virial radii of host and satellite as LD is that the number of interlopers can be minimized by constraining the boundary of satellite systems as a physical boundary in which hydrodynamical interactions between host and satellites are expected.

The constraint on ΔV^* is not simple because it should depend on the environment of the satellite systems as well as the mass of host galaxy. However, we assume a fixed value of ΔV^*=500 km s^{-1} for all the host galaxies regardless of their mass and environment. This value of ΔV^*=500 km s^{-1} is different from that adopted by Ann et al. (2008) who searched isolated satellite systems of galaxies with $0.02 < z < 0.047$ and $M_r < -18$. They assumed ΔV^*=1000 km s^{-1} to constrain the neighbor galaxies. We suppose that taking ΔV^*=500 km s^{-1} is a reasonable choice because the sample galaxies are confined to those with $z \lesssim 0.01$ and the rms peculiar velocity of galaxies in the local universe is roughly 500 km s^{-1} (Peebles 1979, 1987).

Table 1
Number of satellites in six sub-types of dwarfs.

host	dS0[a]	dE	dE$_{bc}$	dSph	dE$^{b}_{blue}$	dI
49 E/S0	15 (4)	13	8	10	5 (1)	52
297 Sp/Irr	3 (1)	18	31	14	46 (9)	176

[a] Includes dS0$_p$ galaxies (number in parenthesis);
[b] includes HII region-like BCDs (number in parenthesis).

Thus, we consider a galaxy with M_r is isolated if there is no neighbor galaxy that has absolute magnitude brighter than $M_r + \delta M_r$ with $|\Delta V| < \Delta V^*$ within the projected separation from the host galaxy r_p less than $r_{vir} + r_{virnei}$ where r_{vir} and r_{virnei} are virial radii of the host and its neighbor galaxy, respectively. The virial radius of a galaxy is defined as the radius where the mean density within the sphere centered at the galaxy, $\rho = 3\gamma L/4\pi r_p^3$, becomes the virialized density, which is set to $766\bar{\rho}$ where $\bar{\rho}$ is the mean mass density of the universe (Park et al. 2008). We use the mass-to-light ratio (γ) determined from the $B-V$ colors (Wilkins et al. 2013) which are derived from $g-r$ colors using the transformation equation $B-V = 0.98(g-r)+0.22$ (Jester et al. 2005).

The number of isolated host galaxies selected from 5836 galaxies in the local universe depends on δM_r. After examining several values of δM_r we adopt $\delta M_r = 1.0$ for the present study. It gives 346 isolated satellite systems. Once an isolated host is selected, it is easy to find satellite galaxies that belong to it. This is because all the galaxies satisfying the constraint for the neighbor galaxy are considered to be satellite galaxies if they are located within the LD defined by the sum of the virial radii of the host and satellite. We find 835 satellite galaxies that belong to 346 isolated hosts. Among the 835 satellites, 411 satellites are dwarf galaxies. Table 1 lists the number of satellites in six sub-types of dwarf galaxies sorted by the host morphology. It seems worthwhile to note that the two sub-types, dS0 and dE$_{blue}$, behavior very differently. The majority ($\sim 83\%$) of dS0 satellites belong to early-type host while the majority ($\sim 88\%$) of dE$_{blue}$ belong to late-type host. The dE$_{bc}$ galaxies which we consider as early-types show host distribution similar to the sub-types considered as late-types (dE$_{blue}$ and dI).

We used all the dwarf satellites in Table 1 to derive the surface density and early-type fractions of the satellite systems. However, we did not use the satellite systems which are located close to the boundary of the SDSS survey volume in the derivation of the local background density because the local background densities are supposed to be underestimated near the

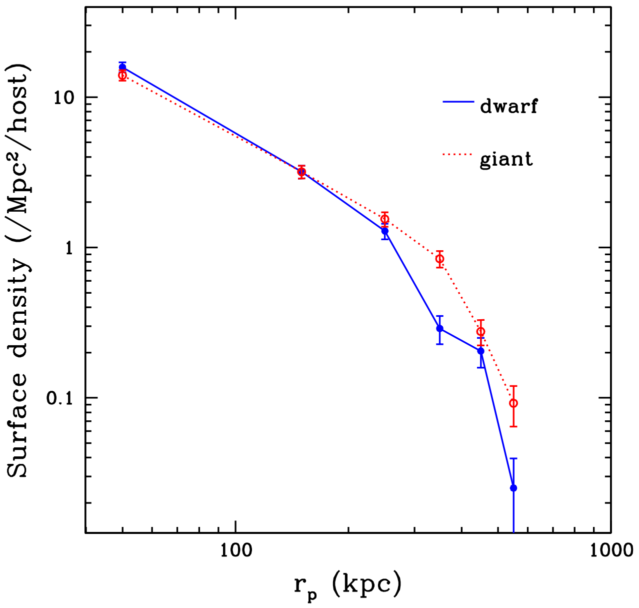

Figure 3. Surface density distributions of dwarf and giant satellites along the galactocentric distance (r_p) from host galaxy. The solid line represents dwarfs and the dotted line indicates giants. Errors are Poisson errors.

survey boundary. There are 22 satellite systems whose distances to the survey boundary are closer than the distances to the 5th nearest galaxies. The 22 satellite systems near the survey boundary are hosted by the late-type galaxies. Among the 22 satellite systems, 9 satellite systems have dwarf satellites. The total number of dwarf satellites in these 9 satellite systems are 10. They are mostly dwarf irregular galaxies. The mean distance to the 5th nearest galaxies for these 9 satellite systems is ~ 1 Mpc.

3. RESULTS

We treat the isolated satellite systems selected by the previous section as an ensemble to examine the radial distribution of satellites because only a few satellite systems have satellites numerous enough to analyze their spatial distribution. The average number of satellites in an isolated satellite system is ~ 2.4 and the number of dwarfs is similar to that of giants.

3.1. Radial Distribution of Satellite Galaxies

3.1.1. Satellite Surface Density

Figure 3 shows the distributions of surface density of dwarf and giant satellites as a function of projected distance from the host galaxy, i.e., galactocentric distance, r_p. The surface density plotted in Figure 3 is the number of satellites in each annulus divided by the annulus area and the number of host galaxies. The width of each annulus is 100 kpc. At first glance, the surface density of satellites decreases outward rapidly with a sharp boundary at $r_p \approx 600$ kpc. The general trend of the surface densities of dwarf and giant satellites is similar to each other except for the more rapid decrease of dwarfs at $r_p > 250$ kpc. The reason for the significantly smaller number of dwarfs than giants at $r_p > 250$ kpc is a natural consequence of the constraint imposed on searching for satellites. We used a variable LD that depends on the virial radii of host and satellite. That is, the limiting separation between the host and its satellite is set by the sum of their virial radii. Since dwarfs have smaller virial radii than giants, they can not be located at large distances from the host galaxy. To check this, we searched satellites by assuming a fixed radius of 500 kpc as the boundary of a satellite system and found that the number of dwarfs in the outer part is close to or larger than the number of giants. However, we suppose that the majority of dwarf satellites found beyond the LD are field galaxies.

Figure 4 shows how the spatial distributions of dwarf satellites vary with the host morphology. We use the r_p/R_{vir} to represent the galactocenteric distance of a satellite galaxy. First of all, what is remarkable is that the surface density of early-type dwarfs is much higher than that of the late-type dwarfs in the innermost regions of the satellite systems hosted by early-type galaxies, while the surface density of early-type dwarfs is lower than that of the the late-type dwarfs in the outer parts of the satellite systems ($r_p/\mathrm{R}_{vir} > 0.6$). Here, we consider the dE, dE_{bc}, dSph and dS0 galaxies as early-type dwarfs, whereas the dI, dE_{blue} and the HII region-like BCDs as late-type dwarfs. Considering that the number of late-type dwarfs is much larger than the early-type dwarfs, the larger numbers of early-type dwarfs in the vicinity of early-type host galaxies imply that a significant fraction of late-type dwarfs are transformed into early-type dwarfs by some mechanisms. This can be ram pressure stripping by the hot corona of early-type host. Tidal stirring by the massive early-type host may play some role inshaping the early-type morphology. On the other hand, in the vicinity of a late-type host, late-type dwarfs are more abundant than early-type dwarfs. The reason for the low surface density of early-type dwarfs near the late-type host is two-fold. One is that the ram pressure from the hot corona of a late-type host is not strong enough to remove the cold gas from late-type dwarfs because the hot corona of late-type galaxies is thought to be smaller and less luminous than that of early-type galaxies (Jeltema et al. 2008; O'Sullivan et al. 2001; Mulchaey & Jeltema 2010; Rasmussen et al. 2009). In general, X-ray bright galaxies are more massive and luminous than X-ray faint galaxies (Forman et al. 2005; Trincheri & Fabbiano 1985; Fabbiano 1989). Thus, the ram pressure stripping and tidal stirring are more effective in satellites belonging to early-type host galaxies. The other reason is that the cold gas in late-type hosts can be transferred to the satellite galaxies if they are close enough to exchange their gas. The high surface density of early-type satellites in the central regions of the systems hosted by early-type galaxies and the low surface density of early-type satellites in the systems hosted by late-type galaxies are the galaxy morphology conformity found in the satellite systems (Ann et

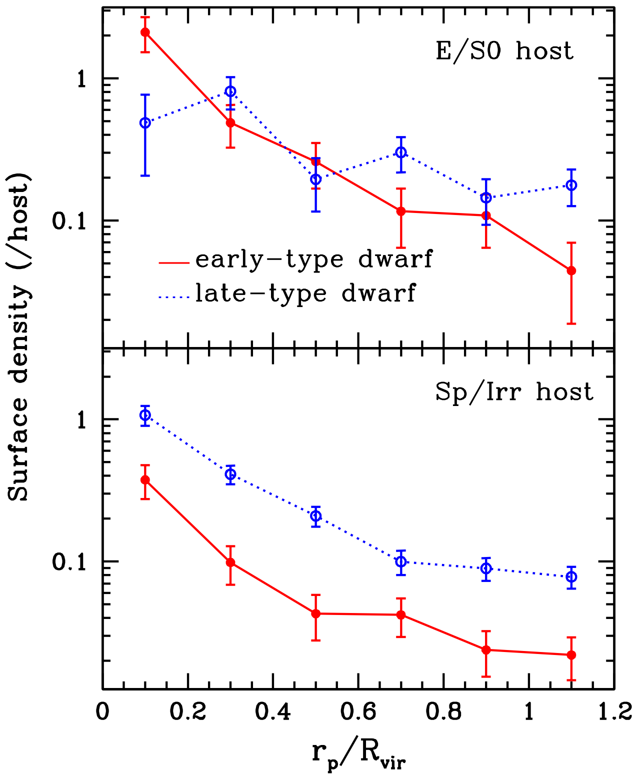

Figure 4. Surface number density of dwarf satellites, sorted by host and satellite morphology, as a function of r_p/R_{vir}. Satellite systems hosted by early-type galaxies are in the upper panel and those hosted by late-type galaxies are in the lower panel. Solid lines represent early-type dwarf satellites and dotted line represent late-type dwarf satellites.

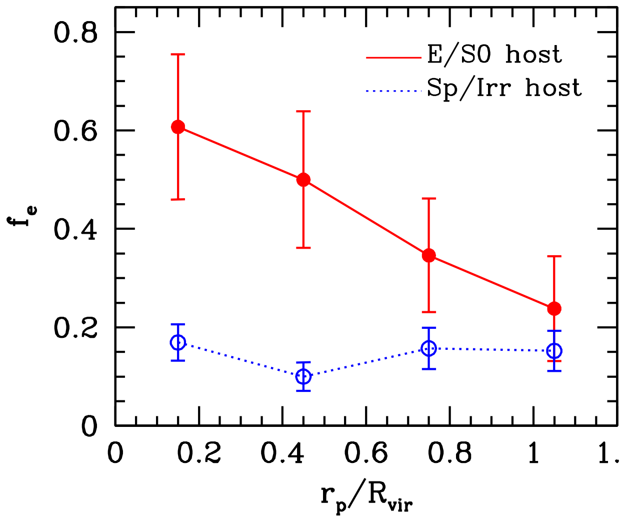

Figure 5. Early-type fractions as a function of r_p/R_{vir}. The early-type fractions of dwarf satellites hosted by early-type galaxies are plotted by a solid line and filled circles while those of dwarf satellites hosted by late-type galaxies are plotted by a dotted line and open circles.

al. 2008). One thing worth noting is that the surface density of the dwarf satellites in the systems with early-type hosts is higher than that of the satellite systems with late-type hosts. The overall higher surface density around the early-type host galaxy is easy to understand if we consider the morphology-density relation (Dressler 1980) and luminosity-density relation (Park et al. 2007) which dictate that massive galaxies are likely to be formed in the high-density regions.

3.1.2. Early Type Fraction of Dwarf Satellites

Since the finding that the morphology of a satellite galaxy is likely to resemble the morphology of its host galaxy (Weinman et al. 2006; Ann et al. 2008; Kauffmann et al. 2013), morphology conformity becomes an important tool to understand the formation of galaxies. The galaxy morphology conformity holds for any two galaxies which are near enough to interact hydrodynamically (Park et al. 2008). However, galaxies in the previous studies are mostly giant galaxies because of the observational data they used. Kauffmann et al. (2013) include dwarf galaxies in their sample but it is limited to dwarf galaxies brighter than $M_r = -16$. Here we present the morphology conformity between the giant host and its dwarf satellites in the isolated satellite systems. In the following, as in Figure 4, we consider the four sub-types of dwarf galaxies (dS0, dE, dE$_{bc}$ and dSph) as early-types and the other two sub-types (dE$_{blue}$ and dI) as late-types. The HII region-like BCDs are combined with the dE$_{blue}$ galaxies because there is no significant difference between them.

Figure 5 shows the early-type fraction f_e of dwarf satellite galaxies as a function of r_p/R_{vir}. It is apparent that the degree of morphology conformity between a host and its satellites decreases with r_p/R_{vir}. At $r_p/R_{vir} \approx 0.15$, the early-type satellite fraction of the early-type host is ~ 0.6 while that of late-type host is ~ 0.2. The degree of galaxy morphology conformity between the host and its dwarf satellites revealed in the isolated satellite systems is stronger than that found in Ann et al. (2008) where satellites are brighter than $M_r = -18$. The difference in f_e between early-type hosts and late-type hosts decreases with r_p/R_{vir} and becomes indistinguishable at $r_p/R_{vir} > 1.2$. Ann et al. (2008) interpreted the morphology conformity found in their sample galaxies ($0.02 < z < 0.047$) as a result of the hydrodynamical interactions between the hot corona gas of the host galaxy and the cold gas in the satellite galaxies, which removes the cold gas from the satellites.

3.1.3. Cumulative Distribution of Dwarf Satellite Galaxies

Since the number of satellite galaxies in the isolated satellite systems analyzed here is not large enough to suppress the statistical noise in the spatial distributions, we analyze their cumulative spatial distribution along the projected galactocentric distance (r_p). Figure 6 shows the cumulative fractions of satellite galaxies grouped by the sub-types as a function of r_p. The upper panel shows the cumulative spatial distributions of satellite galaxies with early-type host galaxies, and the lower panel shows the cumulative spatial distributions

Table 2
K-S test probabilities for six sub-types of dwarf galaxies as function of host type.

Type	dS0	dE	dE$_{bc}$	dSph	dE$_{blue}$	dI
Early type host						
dS0	1.000	0.044	0.038	0.653	0.388	0.740
dE	0.044	1.000	0.008	0.689	0.020	0.024
dE$_{bc}$	0.038	0.008	1.000	0.047	0.181	0.048
dSph	0.653	0.689	0.047	1.000	0.375	0.633
dE$_{blue}$	0.388	0.020	0.181	0.375	1.000	0.355
dI	0.740	0.024	0.048	0.633	0.355	1.000
Late type host						
dS0	1.000	0.690	0.722	0.259	0.540	0.409
dE	0.690	1.000	0.470	0.123	0.219	0.161
dE$_{bc}$	0.722	0.470	1.000	0.709	0.515	0.510
dSph	0.259	0.123	0.709	1.000	0.708	0.601
dE$_{blue}$	0.540	0.219	0.515	0.708	1.000	0.834
dI	0.409	0.161	0.510	0.601	0.834	1.000

of satellite galaxies with late-type host galaxies. The cumulative distribution of satellite galaxies shown in Figure 6 is notable in several respects. First of all, the cumulative distribution of the satellite galaxies along the projected distance varies greatly depending on the type of host galaxy. When the host galaxies are early-types, the cumulative distributions of satellites with different dwarf morphology differ greatly, whereas they are less different, especially in the central regions at $r_p < 0.1$ Mpc, when the host galaxies are late-types. Table 2 shows the probabilities of the K-S test to see the statistical significance of the differences in the spatial distributions of dwarf satellite galaxies. We used the significance level of $\alpha = 0.05$ to test the null hypothesis that the two samples are drawn from the same population. Thus, if the probability of the K-S test is less than 0.05, the spatial distribution of the two samples is thought to be statistically different. For example, for dwarf satellites of early-type galaxies, the spatial distribution of dE satellites is statistically different from those of other dwarf satellites except for dSph, whereas the spatial distribution of dE$_{blue}$ satellites is statistically different from that of dE satellites only. In cases of dwarf satellites of late-type host galaxies, there is no statistical difference between the spatial distributions of dwarf satellite galaxies.

In the case of the dE galaxies, the spatial distribution is most centrally concentrated in the satellite systems hosted by early-type galaxies while they are less centrally concentrated than dE$_{bc}$, dE$_{blue}$ and dI galaxies in the satellite systems hosted by the late-type galaxy. The dSph satellite galaxies show a spatial distribution similar to that of the dE galaxy with a slightly less central concentration with the early-type host and a slightly higher central concentration with the late-type host, especially at $r_p < 0.2$ Mpc. The difference in the spatial distributions of dE and dSph galaxies in the satellite systems hosted by early-type galaxies and late-type galaxies is very natural if cold gas can be removed from satellite galaxies or transferred from host to satellite by hydrodynamical interactions between host and satellite (Rafieferantsoa et al. 2009). Cold gas in the progenitors of dE and dSph satellites lying close to the early-type host can be easily removed by interaction with the early-type host which have a large hot corona to make dE and dSph galaxies. The dE and dSph galaxies at a large distance from late-type hosts might be formed with the present morphology and could keep their morphology because of the weak interactions with the host galaxy. The removal of cold gas of dE and dSph satellites by the hot halo gas in host galaxies, especially for early-type hosts, seems to be consistent with the anti-correlation between the HI content and the halo mass (Stark et al. 2016; Brown et al. 2017).

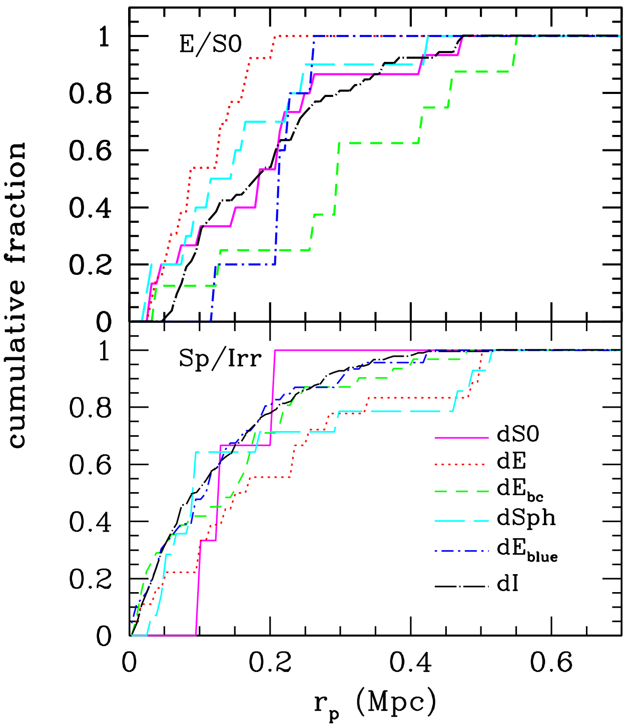

Figure 6. Cumulative fraction of dwarf satellites as a function of r_p. Satellite systems hosted by early-type galaxies are in the upper panel and those hosted by late-type galaxies are in the lower panel. The cumulative fractions of the five sub-types of dwarf elliptical-like galaxies and dwarf irregular galaxies are plotted by different lines: solid line (dS0), dotted line (dE), short-dashed line (dE$_{bc}$), long-dashed line (dSph), dot and short-dashed line (dE$_{blue}$), and dot and long dashed line (dI).

The spatial distribution of dE$_{bc}$ galaxies is of special interest. In the satellite systems hosted by early-type galaxies, the dE$_{bc}$ galaxies show a spatial distribution which is significantly different from that of other dwarf galaxies. The cumulative fractions of other dwarf satellites in early-type hosts are greater than $\sim 60\%$ at $r_p \approx 0.2$ Mpc, whereas the cumulative fraction of dE$_{bc}$ galaxies is only $\sim 25\%$ at the same radius. More than half of the dE$_{bc}$ satellites of early-type galaxies are located at $r_p > 0.25$ Mpc. Their spatial distribution is thought to be closely related to their structural properties, i.e., young stellar populations at the center of galaxies, indicating current star formation and cold gas there. However, since the amount of cold gas in dE$_{bc}$ satellites is not supposed to be large enough to maintain star formation for a long time, it seems plausible that the cold gas is recently accreted from the outside similar to some dE$_{bc}$ galaxies in the Virgo cluster (Hallenbeck et al. 2012). The presence of young stellar populations in the central regions of dE$_{bc}$ galaxies, imposes some constraints on their environment. They should be located in the regions far from the early-type host galaxies to avoid the ram pressure stripping. In cases of the dE$_{bc}$ satellites of late-type galaxies, they can be located close enough to be affected by the ram pressure of the hot corona of host galaxies because cold gas can be transferred from the late-type host. Moreover, the ram pressure from the hot corona of late-type galaxies is less than that of the early-type galaxies because their X-ray luminosity is less luminous than early-type galaxies (Forman et al. 2005; Trincheri & Fabbiano 1985; Fabbiano 1989). The spatial distribution of dE$_{bc}$ galaxies shown in Figure 6 seems to supports the constriant for the location of dE$_{bc}$ satellites to keep their cold gas.

The dE$_{blue}$ galaxies in the satellite systems hosted by early-type galaxies show a very narrow range of distribution. They exist only at 0.1 Mpc $< r_p <$ 0.3 Mpc. Since the number of dE$_{blue}$ galaxies in these systems is so small, only five galaxies, the narrow spatial distribution may be due to the poor statistics, However, the absence of dE$_{blue}$ galaxies at $r_p <$ 0.1 Mpc seems to be a real feature because cold gas in a small system such as a dE$_{blue}$ galaxy can not survive inside the hot dense corona of early-type galaxies. This is plausible because the hot corona of early-type galaxies seems to extend to $\sim$ 0.1 Mpc (Forman et al. 2005). On the other hand, the absence of dE$_{blue}$ galaxy at $r_p >$ 0.3 Mpc is simply due to the small number statistics. In the satellite systems hosted by late-type galaxies, the distribution of dE$_{blue}$ galaxies is nearly identical to that of dI galaxies and similar to that of dE$_{bc}$ galaxies. The common property of these three sub-types of dwarf galaxies is the presence of cold gas.

3.2. Background Density Dependence

As we have seen in the previous section, the spatial distributions of satellite galaxies around host galaxy depend on the morphology of host and satellite. The dependence of satellite morphology on the galactocentric distance (r_p) seems to be related to the local background density while the dependence of satellite morphology on the host morphology is related to the global background density. This is because there is a clear correlation between r_p and the local background density in groups and clusters (Dressler 1980; Whitmore & Gilmore 1991) and host morphology depends on the background density, probably global density, via the morphology-density relation (Dressler 1980).

The background density of a galaxy can be defined by several ways (Muldrew et al. 2012). We adopt the nth nearest neighbor method to calculate the background density of dwarf satellites. In the nth nearest neighbor method, the background density Σ_n of a target galaxy is calculated using the following equation,

$$\Sigma_n = \frac{n}{\pi r_{p,n}^2}$$

where $r_{p,n}$ is the projected distance from a target galaxy to the nth nearest neighbor galaxy. There are two constraints for selecting the neighbor galaxies for the derivation of the background density. One is the limiting magnitude ($M_r{}^*$) of galaxies to be searched for, and the other is the linking velocity (ΔV^*) between the target galaxy and its neighbors. We used two values of $M_r{}^*$. One is $M_r{}^* = -15.2$ which is the absolute magnitude of a galaxy with an apparent magnitude $r = 17.77$ at $z = 0.01$ and the other is $M_r{}^* = -20.6$ which corresponds to the absolute magnitude of L^* galaxies for the Schechter luminosity function fitted to the SDSS galaxies at $z < 0.01$ (Ann et al. 2015). We adopt ΔV^*=1000 km s^{-1}. For n, there is no physical ground to select n, but, as Muldrew et al. (2012) demonstrated, a small value of n yields a high spatial resolution but with a low signal-to-noise ratio while a large value of n gives rise to a smoothed local background density with a low spatial resolution. We used $n = 5$ for both values of $M_r{}^*$. The background density derived with $M_r{}^* = -15.2$ gives a higher spatial resolution than that derived with $M_r{}^* = -20.6$. We use the terminology local background density (Σ_L) and global background density (Σ_G) for the background densities derived with $M_r{}^* = -15.2$ and $M_r{}^* = -20.6$, respectively. The mean distances to the 5th nearest neighbor galaxies are 0.65 Mpc and 9.7 Mpc, respectively for Σ_L and Σ_G.

Figure 7 shows the cumulative fraction of dwarf satellites as a function of the background density normalized by the mean background density ($\Sigma/\bar{\Sigma}$). The local background density (Σ_L) is plotted in the upper panel and the global background density (Σ_G) in

Table 3
K-S test probabilities for six sub-types of dwarf galaxies as function of background density.

Type	dS0	dE	dE$_{bc}$	dSph	dE$_{blue}$	dI
			local background density			
dS0	1.000	0.617	0.436	0.615	0.031	0.026
dE	0.617	1.000	0.035	0.144	0.000	0.000
dE$_{bc}$	0.436	0.035	1.000	0.283	0.027	0.007
dSph	0.615	0.144	0.283	1.000	0.059	0.047
dE$_{blue}$	0.031	0.000	0.027	0.059	1.000	0.111
dI	0.026	0.000	0.007	0.047	0.111	1.000
			global background density			
dS0	1.000	0.000	0.057	0.001	0.031	0.032
dE	0.000	1.000	0.038	0.666	0.023	0.003
dE$_{bc}$	0.057	0.038	1.000	0.283	0.432	0.621
dSph	0.001	0.666	0.283	1.000	0.171	0.037
dE$_{blue}$	0.031	0.023	0.432	0.171	1.000	0.125
dI	0.032	0.003	0.621	0.037	0.125	1.000

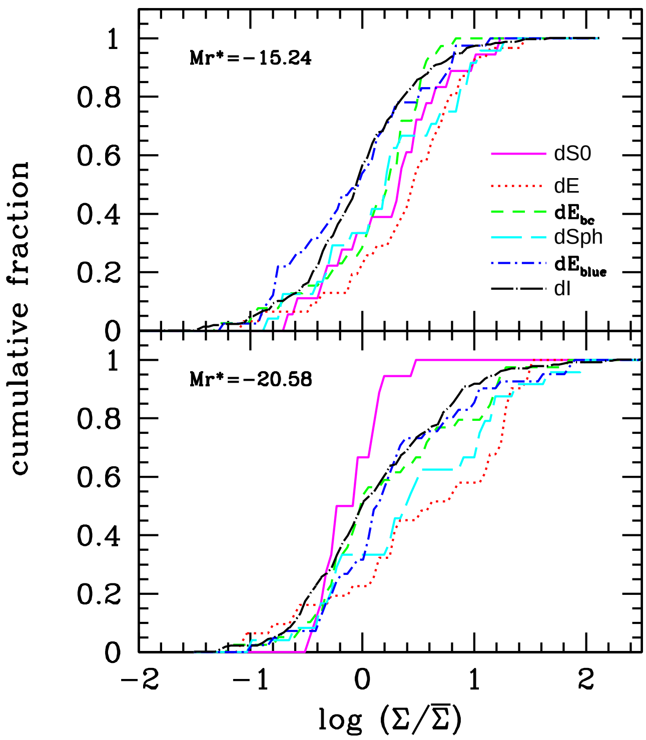

Figure 7. Cumulative fraction of dwarf satellites as a function of Σ. The background density of local environment (Σ_L) is presented in the upper panel and that for the global environment (Σ_G) is given in the lower panel. The cumulative fractions of the five sub-types of dwarf elliptical-like galaxies and dwarf irregular galaxies are plotted by different lines: solid line (dS0), dotted line (dE), short-dashed line (dE$_{bc}$), long-dashed line (dSph), dot and short-dashed line (dE$_{blue}$, and dot and long dashed line (dI).

Table 4
K-S test probabilities for dwarf satellites of late-type hosts.

Type	dS0	dE	dE$_{bc}$	dSph	dE$_{blue}$	dI
			local background density			
dS0	1.000	0.034	0.057	0.053	0.329	0.183
dE	0.034	1.000	0.192	0.690	0.004	0.001
dE$_{bc}$	0.057	0.192	1.000	0.261	0.058	0.024
dSph	0.053	0.690	0.261	1.000	0.016	0.011
dE$_{blue}$	0.329	0.004	0.058	0.016	1.000	0.274
dI	0.183	0.001	0.024	0.011	0.274	1.000
			global background density			
dS0	1.000	0.056	0.460	0.095	0.393	0.576
dE	0.056	1.000	0.024	0.375	0.000	0.000
dE$_{bc}$	0.460	0.024	1.000	0.300	0.650	0.498
dSph	0.095	0.375	0.300	1.000	0.046	0.011
dE$_{blue}$	0.393	0.000	0.650	0.046	1.000	0.089
dI	0.576	0.000	0.498	0.011	0.089	1.000

the lower panel. There are some differences in the cumulative distributions of Σ_L between early-type satellites (dS0, dE, dSph, and dE$_{bc}$) and late-type satellites (dE$_{blue}$ and dI). However, as shown in the probability of the K-S test in Table 3, the majority of these differences are statistically insignificant because they have probability larger than the significance level of $\alpha = 0.05$. Among the early-type dwarf satellites, dS0, dE, and dE$_{bc}$ galaxies have Σ_L significantly different from those of late-type dwarfs (dE$_{blue}$ and dI). The Σ_L distribution of dSph galaxies are significantly different from dI galaxies but the significance level is marginal for dE$_{blue}$ galaxies. It is of interest to see the Σ_L distribution of dE$_{bc}$ galaxies. It is significantly different from dE galaxies as well as dE$_{blue}$ and dI galaxies. This means that they are likely to be located in the regions with intermediate local background density.

On the other hand, the distributions of Σ_G show no such a division between early-type dwarfs and late-type dwarfs due to different Σ_G distributions of dS0 and dE$_{bc}$ satellites. In particular, the dS0 satellites have a narrow range of Σ_G, confined to $-0.5 < \log(\Sigma_G/\bar{\Sigma}_G) < 0.5$, which makes their Σ_G much different from others. The dE$_{bc}$ satellites have Σ_G similar to dE$_{blue}$ and dI. Since Σ_G reflects the galaxy distribution associated with the large scale structures while Σ_L reflects the galaxy distribution nearby, i.e., galaxies in and around the satellite system they belong to, it is of interest to understand why the two background densities, Σ_L and Σ_G, of dS0 satellites are so different. The dE$_{bc}$ satellites also show quite different density distributions for Σ_L and Σ_G. The Σ_L distribution of dE$_{bc}$ satellites is similar to that of dSph satellites except for an excess near $\log(\Sigma_L/\bar{\Sigma}_L) = 0.7$ while the Σ_G of dE$_{bc}$ satellites is similar to that of dE$_{blue}$ and dI of which $\sim 60\%$ are located in the under-dense regions ($\Sigma_G < \bar{\Sigma}_G$).

Figure 8 shows the cumulative distributions of the dwarf satellites divided into the host galaxy morphology as a function of the background densities, Σ_L in the left panels and Σ_G in the right panels. There is a large difference between the Σ_L and Σ_G. The mean Σ_L of the satellites of early-type galaxies is similar to that of late-type galaxies, whereas the mean Σ_G of satellites of late-type galaxies is much higher than that of the early-type galaxies if we ignore the dS0 satellites of late-type galaxies. On average, the fraction of satellites of early-type galaxies located in the under-dense regions ($\Sigma_G < \bar{\Sigma}_G$) is ~ 0.6 while the fraction of satellites of late-type galaxies located in the under-dense region ($\Sigma_G < \bar{\Sigma}_G$) is ~ 0.3. In the satellite systems hosted by early-type galaxies, the distributions of satellite background densities show no significant difference among the sub-types, whereas in the satellite systems hosted by late-type galaxies, there are significant differences between early-type satellites and late-type satellites if we exclude the dS0 galaxies which have a narrow range of the local background densities around $\log(\Sigma_L/\bar{\Sigma}_L) \approx -0.5$. This feature is more pronounced in the distributions of the global background densities (Σ_G) where we see that the Σ_G of dE and dSph satellites of late-type galaxies are significantly different from those of dE$_{blue}$ and dI satellites. The dE$_{bc}$ satellites

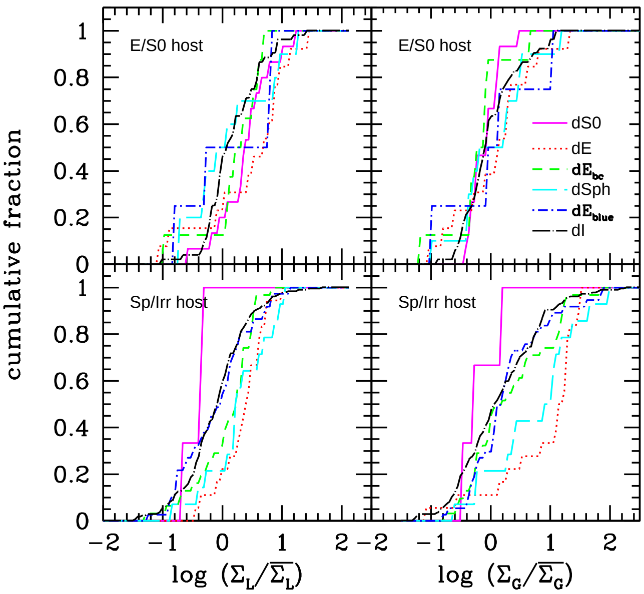

Figure 8. Cumulative fraction of dwarf satellites as a function of $\log(\Sigma/\bar{\Sigma})$. Σ_L is given in the left panels and Σ_G in the right panels. Satellites in early-type hosts are presented in the upper panels while those for late-type hosts are displayed in the lower panels. The cumulative fractions of the five sub-types of dwarf elliptical-like galaxies and dwarf irregular galaxies are plotted by different lines: solid line (dS0), dotted line (dE), short-dashed line (dE$_{bc}$), long-dashed line (dSph), dot and short-dashed line (dE$_{blue}$), and dot and long dashed line (dI).

show Σ_G distribution similar to late-type satellites. We summarize the results of the K-S test to show the significance of the differences between the sub-types of dwarf satellite galaxies in Table 4. We omit the results for the satellites of early-type hosts because there is no significant difference at all. The Σ_G distribution of dE$_{bc}$ satellites may be related to the origin of the cold gas in the central regions of dE$_{bc}$ galaxies. That is, if the cold gas of dE$_{bc}$ satellites is accreted from the intergalactic medium, dE$_{bc}$ galaxies are likely to be found in the regions where cold gas are abundant. We suppose that cold gas is more abundant in the under-dense regions than in the over-dense regions.

The dependence of the background densities on the host and satellite morphology, demonstrated as the differences in the distributions of the background densities shown in Figure 8, implies that the main mechanism to determine the satellite morphology depends on the host morphology as well as the background densities of satellites. The morphology of a satellite of an early-type host galaxy seems to be mostly determined by the interactions with the host galaxy while the morphology of a satellite of a late-type host is more affected by the environment where they formed. The difference between Σ_L and Σ_G of satellites hosted by early-type galaxies seem to be caused by the relative importance of local and global background densities compared with the effect of interactions between host and satellites. The hydrodynamical and tidal interactions between host and satellites seem to be the main cause that determines the morphology of a satellite around an early-type host but the local environment, represented by Σ_L, may affect the satellite morphology somewhat. On the contrary, the global environment, represented by Σ_G, does not affect the satellite morphology in the systems hosted by early-type galaxies.

On the other hand, the satellite morphology seems to be significantly affected by the local and global background densities in the satellite systems hosted by late-type galaxies. If we exclude the dS0 satellites of late-type hosts (three galaxies only), there is a clear difference in the distribution of the background densities between early-type satellites and late-type satellites. In particular, the distribution of Σ_G of dE and dSph satellites are significantly different from those of dE$_{blue}$ and dI satellites. It suggests that most dE and Sph satellites of late-type galaxies, which are located at large galactocentric distances, may have their current morphology before they fall into the satellite system. They may be primordial ones formed in the dense regions in the early history of galaxy formation or they got the current morphology by the frequent interactions with neighbor galaxies, expected in the dense regions.

The argument that early-type satellites, dE and dSph in particular, of early-type galaxies are transformed from late-type galaxies (spirals and irregulars) after they fall into the satellite systems and dE and dSph satellites of late-type galaxies have the current morphology before they come into the satellite systems is supported by their spatial distributions shown in Figure 6. More than 70% of dE and dSph satellites of early-type galaxies are located at $r_p < 0.15$ Mpc where strong hydrodynamical and tidal interactions between the host and satellites are expected. It is highly contrasted with the spatial distributions of dE and dSph satellites of late-type galaxies which show that $\sim$ 30% of dE and dSph galaxies are located at $r_p > 0.25$ Mpc where we expect little interaction between host and satellites.

4. Summary and Discussion

We have studied the dependence of satellite morphology on the environment represented by the projected distance from host galaxy (r_p) and the background densities (Σ) derived by the nth nearest neighbor method using the visually classified morphological types of the nearby galaxies at $z \lesssim 0.01$ (Ann et al. 2015). We have derived a sample of isolated satellite systems using variable linking distance (LD) and fixed linking velocity of $\Delta V^* = 500$ km s^{-1}. The LD we used is the sum of the virial radii of host and satellite. The use of variable LD and a fairly small value of ΔV^* allows us to minimize the inclusion of interlopers in our satellite sample. The number of isolated satellite systems and the number of satellites therein depend on the constraints for the isolation of host galaxies. We consider a galaxy is an isolated host galaxy if there is no neighbor galaxy that has a comparable luminosity, i.e., no neighbor galaxy with $M_r < M_{r,host} + \delta M$ within $r_p = r_{vir} + r_{virnei}$. The number of isolated satellite systems using $\delta M = 1$ is 346 and the mean number of satellites in an isolated satellite system is 2.4. We have explored other values of δM such as 0.5, 1.2, and 1.5 to see the effect of δM on the correlation between the satellite morphology and its environment and found that δM between 0.5 and 1.5 does not affect the results significantly.

We have found that the detailed morphologies of dwarf satellite galaxies depend strongly on the host morphology and r_p. The local background density, derived from galaxies brighter than $M_r = -15.24$ which is the absolute magnitude of a galaxy with $r = 17.77$ at $z = 0.01$, seems to play no significant role for the morphology of dwarf satellite galaxies. However, the global background density, derived from galaxies brighter than $M_r = -20.58$, which corresponds to the absolute magnitude of the L^* galaxy in the luminosity function of the local galaxies ($z < 0.01$) seems to affect the morphology of dwarf satellites of late-type galaxies. The global background density of dE$_{bc}$ satellites similar to dE$_{blue}$ and dI satellites rather than dE and dSph satellites. Since dE$_{bc}$ and dE galaxies have similar luminosities which are on average $\sim$ 1.5 mag brighter than those of dE$_{blue}$ and dI galaxies, the environment, represented by the background densities, plays more significant role on the morphology of dwarf satellites than the mass of dwarf satellites.

The spatial distribution of dwarf satellites suggests that the environmental quenching driven by the ram pressure stripping (Gunn & Gott 1972) of the cold gas in satellite galaxies is operating in the dwarf satellites, especially for the dwarf satellites of the early-type galaxies. The tidal stirring of stars of satellites (Mayer et al. 2001) may change the structure of galaxies from disk shapes to ellipsoidal/spheroidal shapes. This is the reason why dE and dSph galaxies are preponderant in the vicinity of early-type host galaxies. The local and global background densities of dwarf satellites of early-type galaxies are irrelevant to the satellite morphology. On the other hand, a significant fraction of dE and dSph satellites of late-type galaxies seems to be primordial or pre-processed objects because they are located in the outer parts of the satellite systems where environmental quenching is supposed to be ineffective.

Among the satellite spatial distributions, the spatial distribution of dE$_{bc}$ satellites of early-type galaxies is of special interest because it may suggest the origin of the cold gas and the dominant mechanisms for the environmental quenching in the isolated satellite systems. The dE$_{bc}$ galaxies are characterized by the blue core which indicates the presence of the young stellar populations that require cold gas. There are two explanations for the origin of the cold gas in the dE$_{bc}$ satellites if we exclude the recycled gas due to stellar evolution which seems to be less likely (Hallenbeck et al. 2012). One is the leftover material after transformation from late-type galaxies to dE-looking galaxies and the other is the intergalactic material accreted after they formed as dE galaxies (Hallenbeck et al. 2012). Accreted cold gas can fall into the center of a dwarf galaxy without being evaporated by the hot corona gas (Nipoti & Binney 2007). The most pronounced feature of their spatial distribution is the preponderance of dE$_{bc}$ satellites in the outer parts of the satellite systems, more than $\sim$ 60% of dE$_{bc}$ satellites at $r_p > 0.3$ Mpc. This preference of outlying locations for the dE$_{bc}$ satellites of early-type galaxies is consistent with the locations of the dE$_{bc}$ galaxies in the Virgo cluster (Hallenbeck et al. 2012). If they are leftover material which survives from the ram pressure of the hot corona of early-type hosts owing to their large separation from the host galaxies, we do not expect any dependence of dE$_{bc}$ satellites on the background density. On the other hand, if the cold gas are intergalactic material accreted before or after becoming the satellites of early-type galaxies, we expect some dependence of dE$_{bc}$ satellites on the background density. In this regard, the global density distribution of dwarf satellites of early-type galaxies, shown in the upper-right panel of Figure 8, seems to be informative. The fraction of galaxies that have a global background density smaller than the mean value is largest for dE$_{bc}$ satellites ($\sim$ 85%). This fraction of dE$_{bc}$ satellites is about two times larger than that of dE satellites. Thus, it seems more plausible to assume that the cold gas in dE$_{bc}$ satellites is the accreted intergalactic material. We further suppose that most of dE$_{bc}$ satellites become satellites of early-type galaxies recently because the amount of cold gas is not large enough to last for a long time. The spatial distribution of dE$_{bc}$ satellites, characterized by the preponderance of dE$_{bc}$ satellites in the outer parts of the satellite system, implies that the ram pressure stripping (Gunn & Gott 1972) is operating in the vicinity of early-type hosts. We presume that cold gas in dE-looking satellites is easily removed by the ram pressure of early-type host galaxies when they are close enough. This mechanism is the reason for the lack of dE$_{bc}$ satellites in the vicinity of early-type hosts.

An example of the results of the hydrodynamical interaction between host and satellites is the morphology conformity between host and satellites shown in Figure 5. The hydrodynamical interaction between the hot corona gas of a host galaxy and the cold gas of satellite, especially in the satellite systems hosted by early-type galaxies, removes the cold gas from the satellites to transform star forming late-type galaxies into quiescent early-type ones. Tidal interactions play a critical role on transforming the disk-like structure into ellipsoidal/spheroidal shapes. The lack of dE$_{blue}$ galaxies at $r_p < 0.1$ Mpc from early-type hosts also demonstrates the importance of the hydrodynamical interactions in the satellite systems when a host galaxy has a large hot corona which is expected to be present in luminous early-type galaxies. The hydrodynamical interaction between a late-type host galaxy and its satellites, which leads to ram pressure stripping of cold gas in the satellite galaxies, seems to be less effective because the hot corona of the late-type galaxy is less luminous than that of the early-type galaxy.

Acknowledgments

This work was supported partially by the NRF Research grant 2015R1D1A1A09057394.

References

Abadi, M. G., Moore, B., & Bower, R. G. 1999, Ram Pressure Stripping of Spiral Galaxies in Clusters, MNRAS, 308, 947

Abazajian, K. N., et al. 2009, The Seventh Data Release of the Sloan Digital Sky Survey, ApJS, 182, 543

Ann, H. B., Park, C., & Choi, Y.-Y. 2008, Galactic satellite Systems: Radial Distribution and Environment Dependence of Galaxy Morphology, MNRAS, 389, 86

Ann, H. B., Seo, M., & Ha, D. K. 2015, A Catalog of Visually Classified Galaxies in the Local ($z \sim 0.01$) Universese, ApJS, 217, 27

Barazza, F. D., Binggeli, B., & Jerjen, H. 2002, More Evidence for Hidden Spiral and Bar Features in Bright Early-Type Dwarf Galaxies, A&A, 391, 823

Bekki, K. 2009, Ram-Pressure Stripping of Halo Gas in Disc Galaxies: Implications for Galactic Star Formation in Different Environments, MNRAS, 399, 2221

Bekki, K., Couch, W. J., & Shioya, Y. 2002, Passive Spiral Formation from Halo Gas Starvation: Gradual Transformation into S0s, ApJ, 577, 651

Bekki, K., & Couch, W. J. 2011, Transformation from Spirals into S0s with Bulge Growth in Groups of Galaxies, MNRAS 415,1783

Benson, A. J., Toloba, E., Mayer, L., Simon, J. D., & Guhathakurta, P. 2015, Trends in Dwarf Early-Type Kinematics with Cluster-Centric Radius Driven by Tidal Stirring, ApJ, 799, 171

Boselli, A., & Gavazzi, G. 2006, Environmental Effects on Late-Type Galaxies in Nearby Clusters, PASP, 118, 517

Book, L. G., & Benson, A. J. 2010, The Role of Ram Pressure Stripping in the Quenching of Cluster Star Formation, ApJ, 716, 810

Boselli, A., Boissier, S., Cortese, L., & Gavazz1, G. 2008, The Origin of Dwarf Ellipticals in the Virgo Cluster, ApJ, 674, 742

Brown, T., Catinella, B., Cortese, L., Lagos, C. del P., Dave, R., Kilborn, V., Haynes, M. P., Giovanelli, R., & Rafieferantsoa, M. 2017, Cold Gas Stripping in Satellite Galaxies: From Pairs to Clusters, MNRAS, 466, 1275

Chen, J., Kravtsov, A. V., Prada, F., Sheldon, E. S., Klypin, A. A., Blanton, M., Brinckmann, J., & Thakar, A. R. 2006, Constraining the Projected Radial Distribution of Galactic Satellites with the Sloan Digital Sky Survey, ApJ, 647, 86

Choi, Y.-Y., Han, D.-H., & Kim, S. S. 2010, Korea Institute for Advanced Study Value-Added Galaxy Catalog, JKAS, 43,191

Davies, R. L., Efstathiou, G., Fall, S. M., Illingworth, G., & Schechter, P. L. 1983, The Kinematic Properties of Faint Elliptical Galaxies, ApJ, 266, 41

Dressler, A. 1980, Galaxy Morphology in Rich Clusters - Implications for the Formation and Evolution of Galaxies, ApJ, 236, 351

Emerick, A., Mac Low, M.-M., Grcevich, J., & Gatto, A. 2016, Gas Loss by Ram Pressure Stripping and Internal Feedback from Low-Mass Milky Way Satellites, ApJ, 826, 148

Eskridge, P. B. 1988, Physical Constraints on the Production of Extreme Dwarf Ellipticals via Ram-Pressure Stripping - A Test Case in the M81 Group, Astrophys. Lett. Commun., 26, 315

Fabbiano, G. 1989, X-Rays from Normal Galaxies, ARA&A, 27, 87

Ferguson, H. C., & Binggeli, B. 1994, Dwarf Elliptical Galaxies, A&ARv, 6, 67

Fillingham, S. P., Cooper, M. C., Pace, A. B., Boylan-Kolchin, M., Bullock, J. S., Garrison-Kimmel, S., & Wheeler, C. 2016, Under Pressure: Quenching Star Formation in Low-Mass Satellite Galaxies via Stripping, MNRAS, 463, 1916

Forman, W., Jones, C., & Tucker, W. 1985, Hot Coronae around Early-Type Galaxies, ApJ, 293, 102

Gatto, A., Fraternali, F., Read, J. I., Marinacci, F., Lux, H., Walch, S. 2013, Unveiling the Corona of the Milky Way via Ram-Pressure Stripping of Dwarf Satellites, MNRAS, 433, 2749

Gallagher, J. S. III, & Wyse, R. F. G. 1994, Dwarf spheroidal galaxies: Keystones of galaxy evolution, PASP, 106, 1225

Geha, M., Guhathakurta, P., & van der Marel, R. P. 2002, Internal Dynamics, Structure, and Formation of Dwarf Elliptical Galaxies. I. A Keck/Hubble Space Telescope Study of Six Virgo Cluster Dwarf Galaxies, AJ, 124, 3073

Geha, M., Guhathakurta, P., & van der Marel, R. P. 2003, Internal Dynamics, Structure, and Formation of Dwarf Elliptical Galaxies. II. Rotating versus Nonrotating Dwarfs, AJ, 126, 1794

Graham, A. W., Jerjen, H., & Guzman, R. 2003, Hubble Space Telescope Detection of Spiral Structure in Two Coma Cluster Dwarf Galaxies, AJ, 126, 1787

Grebel, E. K. 1997, Star Formation Histories of Local Group Dwarf Galaxies. (Ludwig Biermann Award Lecture 1996), Rev. Mod. Astron., 10, 29

Gunn, J. E., & Gott, J. R. III. 1972, On the Infall of Matter Into Clusters of Galaxies and Some Effects on Their Evolution, ApJ, 176, 1

Hallenbeck, G., Papastergis, E., Huang, S., Haynes, M. P., Giovanelli, R., Boselli, A., Boissier, S., Heinis, S., Cortese, L., & Fabello, S. 2012, Gas-Bearing Early-Type Dwarf Galaxies in Virgo: Evidence for Recent Accretion, AJ, 144, 87

Hester, J. A. 2006, Ram Pressure Stripping in Clusters and Groups, ApJ, 647, 910

Haynes, M. P., Giovanelli, R., & Chincarini, G. L. 1984, The Influence of Envirionment on the H I Content of Galaxies, ARA&A, 22, 445

Hopkins, P. F., Hernquist, L., Cox, T. J., Younger, J. D., & Besla, G. 2008, The Radical Consequences of Realistic Satellite Orbits for the Heating and Implied Merger Histories of Galactic Disks, ApJ, 688, 757

Hwang, J.-S., & Park. C. 2015, Effects of Hot Halo Gas on Star Formation and Mass Transfer During Distant Galaxy-Galaxy Encounters, ApJ, 805, 131

Jachym, P., Palous, J., Koppen, J., & Combes, F. 2007, Gas Stripping in Galaxy Clusters: A New SPH Simulation Approach, A&A, 472, 5

Janz, J., Laurikainen, E., Lisker, T., Salo, H., Peletier, R. F., Niemi, S.-M., den Brok, M., Toloba, E., Falcon-Barroso, J., Boselli, A., & Hensler, G. 2012, Dissecting Early-Type Dwarf Galaxies into Their Multiple Components, ApJ, 745, L24

Jeltema, T. E., Binder, B., & Mulchaey, J. 2008, The Hot Gas Halos of Galaxies in Groups, ApJ, 679, 1162

Jerjen, H., Kalnajs, A., & Binggeli, B. 2000, IC3328: A "Dwarf Elliptical Galaxy" with Spiral Structure, A&A, 358, 845

Jester, S., et al. 2005, The Sloan Digital Sky Survey View of the Palomar-Green Bright Quasar Survey, AJ, 130, 873

Kauffmann, G., Li, C., Zhang, W.,& Weinmann, S. 2011, A Re-Examination of Galactic Conformity and a Comparison with Semi-Analytic Models of Galaxy Formation, MNRAS, 430, 1447

Kawata, D., & Mulchaey, J. S. 2008, Strangulation in Galaxy Groups, ApJ, 672, L103

Kimm, T., Yi, S. K., & Khochfar, S. 2011, The Impact of Gas Stripping and Stellar Mass Loss on Satellite Galaxy Evolution, ApJ, 729, 11

Kovac, K., et al. 2014, zCOSMOS 20k: Satellite Galaxies are the Main Drivers of Environmental Effects in the Galaxy Population at Least to $z \sim 0.7$, MNRAS, 438, 717

Karachentsev, I., Kaisina, E. I., & Makarov, DD. I. 2014, Suites of Dwarfs around nearby Giant Galaxies, AJ, 147, 13

Kraan-Korteweg, R. C. 1986, A Catalog of 2810 Nearby Galaxies – The Effect of the Virgocentric Flow Model on Their Observed Velocities, A&AS, 66, 255

Kravtsov, A. V., Gnedin, O. Y., Anatoly, A., & Klypin, A. A. 2004, The Tumultuous Lives of Galactic Dwarfs and the Missing Satellites Problem, ApJ, 609, 482

Larson, R. B., Tinsley B. M., & Caldwell C. N. 1980, The Evolution of Disk Galaxies and the Origin of S0 Galaxies, ApJ, 237, 692

Lisker, T., Grebel, E., & Bingelli, B. 2006, Virgo Cluster Early-Type Dwarf Galaxies with the Sloan Digital Sky Survey. I. On the Possible Disk Nature of Bright Early-Type Dwarfs, AJ, 132, 497

Lisker, T., Grebel, E. K., Bingelli, B., & Glatt, K. 2007, Virgo Cluster Early-Type Dwarf Galaxies with the Sloan Digital Sky Survey. III. Subpopulations: Distributions, Shapes, Origins, ApJ, 660, 1186

Lisker, T. 2009, Early-Type Dwarf Galaxies in Clusters: A Mixed Bag with Various Origins?, AN, 330, 1043

Lokas, E. L., Kazantzidis, S., Klimentowski, J., Mayer, L., & Callegari, S. 2010, The Stellar Structure and Kinematics of Dwarf Spheroidal Galaxies Formed by Tidal Stirring, ApJ, 708, 1032

Makarov, D., & Karachentsev, I. 2011, Galaxy Groups and Clouds in the Local ($z \sim 0.01$) Universe, MNRAS, 412, 2498

Marcolini, A., Brighenti, F., & D'Ercole, A. 2003, Three-Dimensional Simulations of the Interstellar Medium in Dwarf Galaxies - I. Ram Pressure Stripping, MNRAS, 345, 1329

Mateo, M. L. 1998, Dwarf Galaxies of the Local Group, ARA&A, 36, 435

Mayer, L., Governato, F., Colpi, M., Moore, B., Quinn, T., Wadsley, J., Stadel, J., & Lake, G. 2001, The Metamorphosis of Tidally Stirred Dwarf Galaxies, ApJ, 559, 754

Mayer, L., Mastropietro, C., Wadsley, J., Stadel, J., & Moore, B. 2006, Simultaneous Ram Pressure and Tidal Stripping; How Dwarf Spheroidals Lost Their Gas, MNRAS, 369, 1021

McCarthy, I. G., Frenk, C. S., Font, A. S., Lacey, C. G., Bower, R. G., Mitchell, N. L., Balogh, M. L., & Theuns, T. 2008, Ram pressure Stripping the Hot Gaseous Haloes of Galaxies in Groups and Clusters, MNRAS, 383, 593

McKay, T. A., et al. 2002, Dynamical Confirmation of Sloan Digital Sky Survey Weak-Lensing Scaling Laws, ApJ, 571, L85

McKee, C. F., & Begelman, M. C. 1990, Steady Evaporation and Condensation of Isolated Clouds in Hot Plasma, ApJ, 358, 392

Moore, B., Lake G., & Katz, N. 1998, Morphological Transformation from Galaxy Harassment, ApJ, 495, 139

Mould, J. R., et al. 2000, The Hubble Space Telescope Key Project on the Extragalactic Distance Scale. XXVII. A Derivation of the Hubble Constant Using the Fundamental Plane and Dn-sigma Relations in Leo I, Virgo, and Fornax, ApJ, 529, 768

Mulchaey, J., & Jeltema, T. E. 2010, Hot Gas Halos in Early-Type Field Galaxies, ApJ, 715, L1

Muldrew, S. I., et al. 2012, Measures of Galaxy Environment – I. What is 'Environment'?, MNRAS, 419, 2670

Nipoti, C., & Binney, J. 2007, The Role of Thermal Evaporation in Galaxy Formation, MNRAS, 382, 1482

O'Sullivan, E. P., Duncan, A., Forbes, D. A., & Ponman, T. J. 2001, A Catalogue and Analysis of X-Ray Luminosities of Early-Type Galaxies, MNRAS, 328, 461

Park, C., Choi, Y.-Y., Vogeley, M. S., Gott, J. R. III., Blanton, M. R., & SDSS Collaboration. 2007, Environmental Dependence of Properties of Galaxies in the Sloan Digital Sky Survey, ApJ, 658, 898

Park, C., Gott, J. R., & Choi, Y.-Y. 2008, Transformation of Morphology and Luminosity Classes of the SDSS Galaxies, ApJ, 674, 784

Pasetto, S., Chiosi, C., & Carraro, G. 2003, Morphological Evolution of Dwarf Galaxies in the Local Group, A&A, 405, 931

Pedraz, S., Gorgas, J., Cardiel, N., Sanchez-Blazquez, P., & Guzman, R. 2002, Evidence of Fast Rotation in Dwarf Elliptical Galaxies, MNRAS, 332, 59

Peebles, P. J. E. 1979, The Mean Mass Density Estimated from the Kirshner, Oemler, Schechter Galaxy Redshift Sample, AJ, 84, 730

Peebles, P. J. E. 1987, Origin of the Large-Scale Galaxy Peculiar Velocity Field - A Minimal Isocurvature Model, Nature, 327, 210

Peng, Y.-J., et al. 2010, Mass and Environment as Drivers of Galaxy Evolution in SDSS and zCOSMOS and the Origin of the Schechter Function, ApJ, 721, 193

Peng, Y.-J., Lilly, S. J., Renzini, A., & Carollo, M. 2012, Mass and Environment as Drivers of Galaxy Evolution. II. The Quenching of Satellite Galaxies as the Origin of Environmental Effects, ApJ, 757, 4

Prada, F. 2003, Observing the Dark Matter Density Profile of Isolated Galaxies, ApJ, 598, 260

Rafieferantsoa, M., Dave, R., Angles-Alcazar, D., Katz, N., Kollmeier, J. A., & Oppenheimer, B. D. 2015, The Impact of Environment and Mergers on the H I Content of Galaxies in Hydrodynamic Simulations, MNRAS, 453, 3980

Rasmussen, J., Ponman, T. J., & Mulchaey, J. S. 2006, Gas Stripping in Galaxy Groups - The Case of the Starburst Spiral NGC 2276, MNRAS, 370, 453

Rasmussen, J., Sommer-Larsen, J., Pedersen, K., Toft, S., Benson, A., Bower, R. G., & Grove, L. F. 2009, Hot Gas Halos Around Disk Galaxies: Confronting Cosmological Simulations with Observations, ApJ, 697, 79

de Rijcke, S., Dejonghe, H., Zeilinger, W. W., & Hau, G. K. T. 2003, Embedded Disks in Fornax Dwarf Elliptical Galaxies, A&A, 400, 119

Roediger, E., & Hensler, G. 2005, Ram Pressure Stripping of Disk Galaxies. From High to Low Density Environments, A&A, 433, 875

Sales, L., & Lambas, D. G. 2004, Anisotropy in the Distribution of Satellites around Primary Galaxies in the 2dF Galaxy Redshift Survey: the Holmberg effect , MNRAS, 348, 1236

Sales, L., et al. 2007, Satellite Galaxies and Fossil Groups in the Millennium Simulation, MNRAS, 382, 1901

Sandage, A., & Binggeli, B. 1984, Studies of the Virgo Cluster. III - A Classification System and an Illustrated Atlas of Virgo Cluster Dwarf Galaxies, AJ, 89, 919

Slater, C. T., & Bell, E. F. 2014, The Mass Dependence of Dwarf Satellite Galaxy Quenching, ApJ, 792, 141

Stark, D. V., et al. 2016, The RESOLVE Survey Atomic Gas Census and Environmental Influences on Galaxy Gas Reservoirs, ApJ, 832, 126

Strateva, I., et al. 2001, Color Separation of Galaxy Types in the Sloan Digital Sky Survey Imaging Data, AJ, 122, 1861

Tal, T., et al. 2014, Observations of Environmental Quenching in Groups in the 11 GYR since z = 2.5: Different Quenching for Central and Satellite Galaxies, ApJ, 789, 164

Tecce, T. E., Cora, S. A., Tissera, P. B., Abadi, M. G., & Lagos, C. Del P. 2010, Ram Pressure Stripping in a Galaxy Formation Model - I. A Novel Numerical Approach, MNRAS, 408, 2008

Toloba, E., Boselli, A., Cenarro, A. J., Peletier, R. F., Gorgas, J., Gil de Paz, A., & Munoz-Mateos, J. C. 2011, Formation and Evolution of Dwarf Early-Type Galaxies in the Virgo Cluster. I. Internal Kinematics, A&A, 526, 114

Tonnesen, S., & Bryan, G. L. 2009, Gas Stripping in Simulated Galaxies with a Multiphase Interstellar Medium, ApJ, 694, 804

Trinchieri, G., & Fabbiano, G. 1985, A Statistical Analysis of the Einstein Normal Galaxy Sample - Part Two - Elliptical and s0 Galaxies, ApJ, 296, 447

Tully, R. B. 2015, Galaxy Groups, AJ, 149, 54

van den Bergh, S. 1994, The Evolutionary History of Low-Luminosity Local Group Dwarf Galaxies, ApJ, 428, 617

van den Bergh, S. 1999, The Local Group Of Galaxies, A&A Rev., 9, 273

van den Bosch, F. C., Norberg, P., Mo, H. J., & Yang, X. 2004, Probing Dark Matter Haloes with Satellite Kinematics, MNRAS, 352, 1302

van den Bosch, F. C., Yang, X., Mo, H. J., & Norberg, P. 2005, The Abundance and Radial Distribution of Satellite Galaxies, MNRAS, 356, 1233

van Zee L., Skillman, E. D., & Haynes, M. P. 2004, Rotationally Supported Virgo Cluster Dwarf Elliptical Galaxies: Stripped Dwarf Irregular Galaxies?, AJ, 128, 121

Vijayaraghavan, R., & Ricker, P. M. 2015, Ram Pressure Stripping of Hot Coronal Gas from Group and Cluster Galaxies and the Detectability of Surviving X-Ray Coronae , MNRAS, 449, 2312

Vollmer, B. 2009, A Holistic View on Ram Pressure Stripping in the Virgo Cluster. The First Complete Model-Based Time Sequence, A&A, 502, 427

Weinmann, S. M., van den Bosch F. C., Yang X., & Mo, H. J. 2006, Properties of Galaxy Groups in the Sloan Digital Sky Survey - I. The Dependence of Colour, Star Formation and Morphology on Halo Mass, MNRAS, 366, 2

Wetzel, A. R., Tollerud, E. J., & Weisz, D. R. 2015, Rapid Environmental Quenching of Satellite Dwarf Galaxies in the Local Group, ApJ, 808L, 27

Whitmore, B. C., & Gilmore, D. M. 1991, On the Interpretation of the Morphology-Density Relation for Galaxies in Clusters, ApJ, 367, 64

Wilkins, S. M., Gonzalez-Perez, V., Baugh, C. M., Lacey, C. G., & Zuntz, J. 2013, Single-Colour Diagnostics of the Mass-To-Light Ratio - I. Predictions from Galaxy Formation Models, MNRAS, 431, 430

York, D. G., et al. 2000, The Sloan Digital Sky Survey: Technical Summary, AJ, 120, 1579

Yozin, C., & Bekki, K. 2015, The Transformation and Quenching of Simulated Gas-Rich Dwarf Satellites within a Group Environment, MNRAS, 453, 14

Zentner, A. R,, Kravtsov, A. V., Gnedin, O. Y., & Klypin, A. A. 2005, The Anisotropic Distribution of Galactic Satellites, ApJ, 629, 219

Zinger, E., Dekel, A., Kravtsov, A. V., & Nagai, D. 2016, Quenching of Satellite Galaxies at the Outskirts of Galaxy Clusters, arXiv:1610.02644